Binary Copper Carbonyls. Synthesis and Characterization of $Cu(CO)_3$, $Cu(CO)_2$, CuCO, and $Cu_2(CO)_6$

H. Huber, E. P. Kündig, M. Moskovits, and G. A. Ozin*

Contribution from The Lash Miller Chemistry Laboratories and Erindale College, University of Toronto, Toronto, Ontario, Canada. *Received August 24, 1974*

Abstract: The products of the cocondensation reaction of copper atoms with carbon monoxide at 10–15°K are investigated by matrix infrared and uv-visible spectroscopy and are shown to be binary copper carbonyls. Examination of the reaction products in $^{12}C^{16}O$, $^{12}C^{16}O$–$^{13}C^{16}O$, $^{12}C^{16}O$–Ar, $^{12}C^{16}O$–$^{13}C^{16}O$–Ar, and $^{12}C^{16}O$–$^{13}C^{16}O$–$^{12}C^{18}O$–Ar together with matrix warm-up experiments, carbon monoxide and copper concentration dependence studies, as well as experiments involving the simultaneous codeposition of Cu and Ag atoms with CO, establishes the stoichiometries of the complexes to be $Cu(CO)_3$, $Cu(CO)_2$, Cu(CO), and $Cu_2(CO)_6$. Dicopper hexacarbonyl could be synthesized by the matrix dimerization of $Cu(CO)_3$ at 45–50°K or by the reaction of Cu_2 molecules and/or $Cu_2(CO)_n$ complexes with pure CO at 10–15°K. Isotopic frequencies are computed for the CO stretching modes of triangular planar $Cu(CO)_3$ and linear $Cu(CO)_2$ on the basis of the Cotton–Kraihanzel force field approximation and are found to be in close agreement with the observed values. Triple isotope experiments using $^{12}C^{16}O$–$^{13}C^{16}O$–$^{12}C^{18}O$–Ar mixtures are used to characterize CuCO. The data are also used to test the feasibility of probing the mode of bonding of the CO group to the copper. The infrared data for $Cu_2(CO)_6$ are consistent with a structure containing a Cu–Cu bond. Qualitative molecular orbital schemes, consistent with the uv-visible spectroscopic data, are presented for $Cu(CO)_3$ and $Cu_2(CO)_6$. It is proposed that an extremely intense absorption of 417 nm, observed in the electronic spectrum of $Cu_2(CO)_6$, is associated with the σ–σ^* transition between orbitals of the copper–copper bond and as such can be taken as an approximate measure of the strength of the copper–copper bond. Preliminary matrix uv-visible, copper–argon concentration experiments are briefly described and, besides showing copper atoms, yield evidence for the formation of diatomic copper molecules.

The early literature contains many scattered claims for the existence of binary copper carbonyls.[1-3] Most of the experiments were based on the transport properties of heated copper in a stream of CO, the results of which demonstrated that the chances of isolating stable copper carbonyls were extremely slight.[4-7] On the other hand carbon monoxide does weakly chemisorb onto copper films, the infrared CO stretching bands of which suggest bonding to discrete atoms on the surface.[7] The general consensus of opinion suggests that the lack of stability of simple copper carbonyls is a reflection of the stability of a filled 3d valence shell, a situation not conducive to $d_\pi(Cu)$–$\pi^*(CO)$ bonding, in keeping with the observed decrease in charge transfer from the metal into the π^* orbitals of CO on moving to the right of the periodic table.[8]

A technique which is proving useful for obtaining carbonyls which are difficult, if not impossible, to prepare by conventional procedures involves the matrix cocondensation reactions of metal atoms with carbon monoxide at cryogenic temperatures, 4.2–20°K.[9] Some carbonyls that have recently been synthesized and characterized by matrix methods are listed in Table I. Ogden[10] first applied this technique to the copper atom–carbon monoxide matrix reaction and reported preliminary infrared spectroscopic evidence for a copper carbonyl, composition unknown. At about the same time we too were investigating the Cu–CO matrix reaction[11] and had independently arrived at similar conclusions regarding the authenticity of binary copper carbonyls.

The copper–carbon monoxide matrix reaction, however, presented some difficulties relating to the observation that although copper vapor is greater than 99% monatomic under the conditions employed in these experiments,[12] it, like other transition metal vapors,[13] can be induced to react in low temperature matrices with CO to produce either mononuclear or binuclear complexes. Thus we have found it necessary to perform copper concentration dependence studies and mixed copper–silver codeposition experiments to define stoichiometry with respect to copper,[13,17] as well as the normal ligand concentration studies, mixed ligand isotopic substitution, and matrix warm-up experiments used to define ligand stoichiometry. Using these methods in conjunction with matrix isolation infrared and uv-visible spectroscopy, we have been able to obtain evidence for $Cu(CO)_3$, $Cu(CO)_2$, Cu(CO), and $Cu_2(CO)_6$, the latter being the predicted binary carbonyl to follow $Ni(CO)_4$. Furthermore, the copper concentration dependence studies have yielded information on the factors which seem to control the diffusion and dimerization of copper atoms in low temperature matrices.

Experimental Section

Copper was vaporized from a directly heated tantalum cell containing a boron–nitride liner. The furnace used for the evaporation of the copper has been described previously.[14] The rate of copper deposition was continuously monitored by using a quartz crystal microbalance[15] set behind the cell, thereby receiving the backward copper flux. The furnace in which copper and silver were simultaneously vaporized employed a four-electrode system and two quartz crystal microbalances in the same furnace. With this arrangement it was possible to control and monitor the rate of copper and silver deposition into the matrix.

Research grade $^{12}C^{16}O$ (99.99%) and Ar (99.99%) were supplied by Matheson of Canada and $^{13}C^{16}O$ (50–55%) by Analytical Supplies (N.J.). Copper (99.99%) and silver (99.99%) were supplied by McKay, N.Y. Gas mixtures were prepared by conventional vacuum line techniques. Matrix gas flows, controlled by a calibrated micrometer needle valve, were usually in the range 0.1–4.0 mmol/hr. In the infrared experiments matrices were deposited on a CsI window cooled to either 15°K by means of an Air Products Displex closed-cycle helium refrigerator or 10°K by an Air Products liquid helium transfer system. Spectra were recorded on a Perkin-Elmer 180 spectrophotometer. In the uv-visible experiments matrices were deposited onto either a LiF or NaCl window cooled to 10–15°K. Spectra were recorded on a Unicam SP 8000 uv-visible spectrophotometer.

As our experiments progressed it was discovered that the product of the Cu–CO reaction was susceptible to photochemical decomposition during warm-up experiments above 20°K, due to the infrared spectrometer globar source. To eliminate this complication, experiments were performed with a germanium uv-visible cutout filter placed in the beam of the infrared spectrometer. With the germanium filter in place, normal matrix warm-up experiments could be performed.

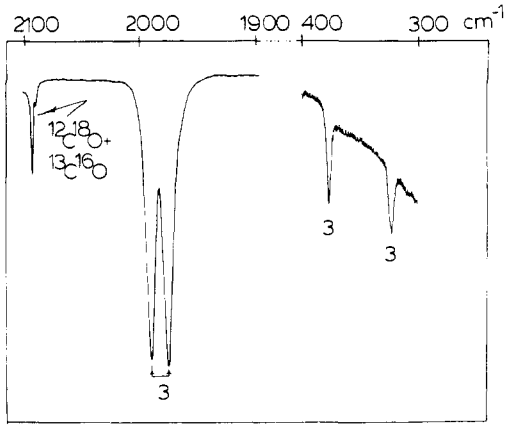

Figure 1. The infrared spectrum of the products of the matrix cocondensation reaction of copper atoms with pure CO at 10–15°K showing the CO stretching and CuC stretching portions of the spectrum.

Table I. Summary of New Mononuclear Carbonyls Synthesised by Metal Atom–Carbon Monoxide Matrix Reactions

Carbonyl	Coordination no., n	Ref
$Ni(CO)_n$	1–4	32
$Pd(CO)_n$	1–4	33, 34
$Pt(CO)_n$	1–4	35
$Co(CO)_n$	1–4	36
$Rh(CO)_n$	1–4	36
$Ir(CO)_n$	1–4	36
$Cr(CO)_n$	1–6	37
$Ta(CO)_n$	1–6	32
$U(CO)_n$	1–6	39
$La(CO)_n$	1–6	40
$Mn(CO)_n$	1–5	13
$Fe(CO)_n$	1–5	41
$V(CO)_n$	1–6	38
$Re(CO)_n$	1–5	37
$Cu(CO)_n$	1–3	10, *a*
$Ag(CO)_n$	1–3	16
$Au(CO)_n$	1–2	42
$Ge(CO)_n$		43
$Sn(CO)_n$		43
$Al_x(CO)_n$	2	44

[a] This study.

Results and Discussion

Cu–$^{12}C^{16}O$ Reactions. When copper atoms were cocondensed with pure $^{12}C^{16}O$ at 10–15°K under conditions of low copper concentration (Cu:CO ≤ 1:1000), *two* CO stretching modes of approximately equal intensity were observed at 1990.0 and 1976.8 cm^{-1} together with two low frequency modes at 376 and 323 cm^{-1} (Figure 1). That these four lines could be ascribed to a single absorbing species (referred to as species 3) was confirmed by studying the relative intensities of the lines over a wide range of Cu:CO concentrations (1:1000 to 1:100,000). These experiments demonstrated that, within experimental error, the absorbance ratio of the doublet remained invariant.

It was found that in the temperature range 35–45°K the absorbances of the observed bands at 1990.0 and 1976.8 cm^{-1} and 376 and 323 cm^{-1} slowly diminished, retaining the same relative intensities at all times. The warm-up data therefore strengthen the assignment of these four lines to a single species 3. Full details of the matrix kinetics and mechanisms of these warm-up reactions will be reported in detail in a forthcoming publication.[16]

Cu–$^{12}C^{16}O$–Ar Reactions. When copper atoms were cocondensed with dilute $^{12}C^{16}O$:Ar ≃ 1:80 mixtures retaining Cu:Ar ≤ 1:1000, two main CO absorptions were observed

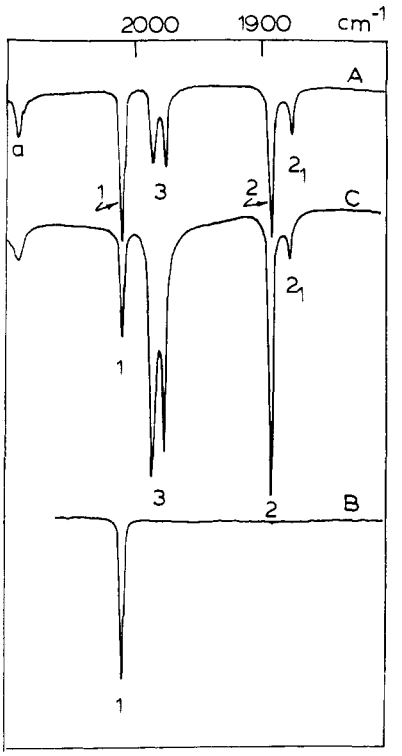

Figure 2. The infrared spectrum of the products of the matrix cocondensation reaction of copper atoms with (A) CO:Ar ≃ 1:80 mixture at 10°K showing $Cu(CO)_3$ (3), $Cu(CO)_2$ (2), Cu(CO) (1), (B) with CO:Ar ≃ 1:500 at 10°K showing Cu(CO) (1), and (C) the same as (A) but after warm-up to 35°K (2_1 represents a matrix splitting of 2 and a represents $^{13}C^{16}O$–$^{12}C^{18}O$ in natural abundance in $^{12}C^{16}O$).

at 2010 and 1891.5 cm^{-1} (labeled 1 and 2, respectively, in Figure 2A) with a weaker doublet at 1985 and 1976 cm^{-1}. On repeating the experiment with more dilute matrices $^{12}C^{16}O$:Ar ≃ 1:500 (retaining the Cu:Ar ≤ 1:1000), a single line was observed at 2010.4 cm^{-1} (Figure 2B), coincident with the line observed in more concentrated matrices, and is assigned to species 1. This absorption under high resolution showed a small splitting, 2010.4 and 2008.3 cm^{-1}, which, from mixed isotope studies, is shown (in a later section) to be a multiple trapping site effect. During warm-up experiments of the 1:80 matrix, in the temperature range 10–35°K, the line labeled 2 grows, followed by the growth of the doublet ascribed earlier to 3. The absorbance of species 1 gradually decreases, leaving 3 and 2 as the major absorbing species (Figure 2C). Warm-up experiments performed on the 1:500 matrices showed similar growth and decay patterns of the lines labeled 3, 2, and 1. It is noteworthy that the doublet splitting for species 3 appears in both pure CO and CO–Ar matrices but is only invariant to annealing in CO matrices (see later section on species 3 in CO matrices).

Carbon Monoxide Mixed Isotope Experiments. Species 3 in CO–Ar Matrices. In argon matrices species 3 shows a doublet absorption in the CO stretching region at 1985 and 1976 cm^{-1}, the $^{12}C^{16}O$–$^{13}C^{16}O$–Ar isotope pattern of which is illustrated in Figure 3 and Tables II and III. Each component of the original doublet absorption can be seen to give rise to an isotope pattern characteristic of a triangular planar tricarbonyl suggesting two slightly different matrix sites for the complex in argon matrices. The vibrational assignments for the tricarbonyl are listed in Table II where the frequency calculations (described in a later section) indicate the presence of an accidental overlap of *one* isotope line of the tricarbonyl in site 3_1 (calcd 1943.0 cm^{-1}) with an intense line of the tricarbonyl in site 3 (obsd 1940.5

Table II. Observed and Calculated Frequencies of Isotopic $Cu(^{12}C^{16}O)_n(^{13}C^{16}O)_{3-n}$ (where $n = 0-3$) in Argon Matrices (Both Sites Included)

Site 3		Site 3_1		
Obsd	Calcd[a]	Obsd	Calcd[a]	Assignment
2079.0	2080.7	2079.0	2084.5	$Cu(^{12}C^{16}O)_2(^{13}C^{16}O)$ (A_1)
2067.0	2066.3	2067.0	2069.9	$Cu(^{12}C^{16}O)(^{13}C^{16}O)_2$ (A_1)
1985.0	1984.9	1975.8	1975.6	$Cu(^{12}C^{16}O)_3$ (E') + $Cu(^{12}C^{16}O)_2(^{13}C^{16}O)$ (B_2)
1966.0	1965.5	1956.8	1956.8	$Cu(^{12}C^{16}O)(^{13}C^{16}O)_2$ (A_1)
1951.5	1951.9	*b*	1943.0	$Cu(^{12}C^{16}O)_2(^{13}C^{16}O)$ (A_1)
1940.5	1940.8	1931.5	1931.7	$Cu(^{13}C^{16}O)_3$ (E') + $Cu(^{12}C^{16}O)(^{13}C^{16}O)_2$ (B_2)
	2091.9		2096.8	$Cu(^{12}C^{16}O)_3$ (A'_1) Raman
	2045.5		2050.2	$Cu(^{13}C^{16}O)_3$ (A'_1) Raman

[a] The best fit CO force constants were: site 3, $K_{CO} = 16.51$, $K_{CO,CO} = 0.59$; site 3_1, $K_{CO} = 16.43$, $K_{CO,CO} = 0.66$ mdyn/Å. Frequencies in cm^{-1}. [b] Hidden by the intense 1940.5-cm^{-1} line of $Cu(CO)_3$ in site 3.

Table III. The Infrared Spectra of $Cu(^{12}C^{16}O)_n(^{13}C^{16}O)_{3-n}$ (where $n = 0-3$) in CO and Ar Matrices

Species 3 in $^{12}C^{16}O-^{13}C^{16}O$ matrices	Species 3 in $^{12}C^{16}O-^{13}C^{16}O$–Ar matrices[a]
1990.0	1985.0
1977.0	
1966.0	1966.0
1961.5	1951.5
1944.0	1940.5
1933.0	

[a] Only the tricarbonyl in site 3 is listed; frequencies are in cm^{-1}.

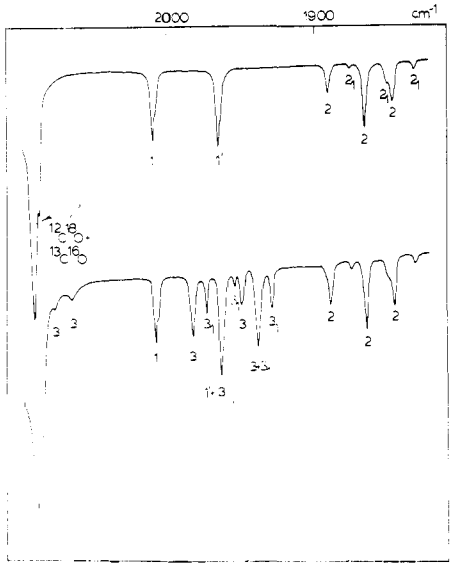

Figure 3. The infrared spectrum of the products of the matrix cocondensation reaction of copper atoms with (A) $^{12}C^{16}O:^{13}C^{16}O:Ar \simeq 1:1:200$ at 10°K and (B) $^{12}C^{16}O:^{13}C^{16}O:Ar \simeq 1:1:200$ after warm-up to 30°K (where the $2/2_1$ and $3/3_1$ notations refer to copper carbonyl species in different matrix sites).

cm^{-1}). Additional experimental evidence which supports the two-site assignment for the tricarbonyl in Ar stems from the observation that, on warming the tricarbonyl in $^{12}C^{16}O-^{13}C^{16}O$-Ar matrices, all of the isotope lines assigned to the tricarbonyl in site 3_1 grow in intensity at the expense of the isotope lines assigned to the tricarbonyl in site 3, both groups of lines maintaining the same relative intensities within a group. The annealing behavior described is typical of a multiple trapping site effect.

Species 1 and 2 in CO–Ar Matrices. To characterize species 1, the experiment was repeated in $^{12}C^{16}O-^{13}C^{16}O$-Ar $\simeq 1-1-1000$ matrices and the spectrum shown in Figure 4 was obtained. The observed isotope pattern confirms that

Table IV. Observed and Calculated Frequencies of Isotopic $Cu(^{12}C^{16}O)_n(^{13}C^{16}O)_{2-n}$ (where $n = 0-2$) in Argon Matrices (Both Sites Included)

Site 2[c]		Site 2_1			
Obsd	Calcd[a]	Obsd	Calcd[a]	Assignment	
b	1995.3	*b*	1994.5	$Cu(^{12}C^{16}O)(^{13}C^{16}O)$	(A_1)
1891.5	1890.8	1876.1	1975.2	$Cu(^{12}C^{16}O)_2$	(Σ_u^+)
1866.0	1866.0	1851.0	1851.0	$Cu(^{12}C^{16}O)(^{13}C^{16}O)$	(A_1)
1848.0	1848.8	1832.5	1833.5	$Cu(^{13}C^{16}O)_2$	(Σ_u^+)

[a] The best fit CO force constants were: site 2, $k_{CO} = 15.41$, $K_{CO,CO} = 0.97$ mdyn/Å; site 2_1, $k_{CO} = 15.29$, $K_{CO,CO} = 1.08$ mdyn/Å. Frequencies are in cm^{-1}. [b] Not observed because of low absorbance. [c] Intensity calculations for isotipic $Cu(^{12}C^{16}O)_n(^{13}C^{16}O)_{2-n}$ (where $n = 0-2$) show that $I_{1995.3}:I_{1890.8}:I_{1866.0}:I_{1848.8} = 3.3:52.8:100:50.5$. These data support the contention that the nonobservation of the out-of-phase CO stretching mode of $Cu(^{12}C^{16}O)(^{13}C^{16}O)$ relates to its low intensity compared to the respective in-phase mode.

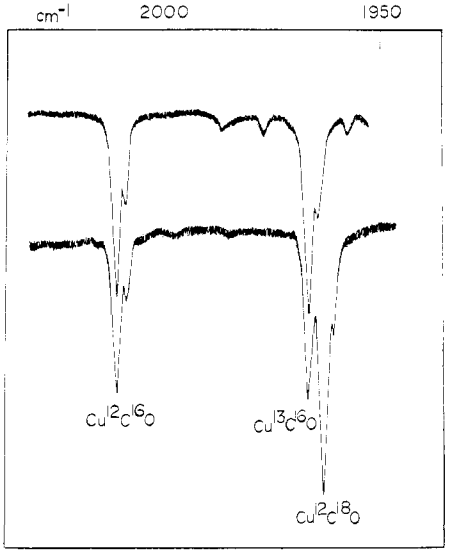

Figure 4. The infrared spectrum of the products of the matrix cocondensation reaction of copper atoms with (A) $^{12}C^{16}O:^{13}C^{16}O:Ar \simeq 1:1:1000$ and (B) $^{12}C^{16}O:^{13}C^{16}O:^{12}C^{18}O:Ar \simeq 1:1:1.5:1500$ at 10°K, showing the presence of $Cu^{12}C^{16}O$, $Cu^{13}C^{16}O$, and $Cu^{12}C^{18}O$.

1 is indeed a monocarbonyl $Cu_y(CO)$. On allowing these dilute $^{12}C^{16}O-^{13}C^{16}O$-Ar = 1-1-1000 matrices to warm up to 30°K, the isotope pattern of species 2 is observed to grow in and is seen to be identical with that observed when 2 is formed from copper atom deposited directly into $^{12}C^{16}O-^{13}C^{16}O$-Ar = 1-1-200 mixtures. The basic pattern (Figure 3 and Table IV) can be identified with that of a dicarbonyl where the single line originally at 1891.5 cm^{-1}, $Cu_z(^{12}C^{16}O)_2$, gives rise to a single counterpart line at

1848.0 cm^{-1}, $Cu_z(^{13}C^{16}O)_2$, with a more intense line at intermediate frequencies 1866.0 cm^{-1}. The latter is assignable to the out-of-phase $^{13}O^{16}O$ stretching mode of $Cu_z(^{12}C^{16}O)(^{13}C^{16}O)$. It is possible that the in-phase $^{12}C^{16}O$ stretching mode for the mixed species is not observed because of its expected low absorbance.

A weak feature at 1876.1 cm^{-1} always appears alongside the 1891.5 cm^{-1} line of 2 and is assigned to a multiple trapping site of 2 (designated 2_1) on the grounds that it too produces an isotope pattern typical of a dicarbonyl but with all lines shifted to slightly lower frequencies than the corresponding lines of 2 (Figure 3 and Table IV).

We can summarize by stating that the information obtained from carbon monoxide mixed isotope experiments establishes that 3, 2, and 1 can be formulated as $Cu_x(CO)_3$, $Cu_y(CO)_2$ and $Cu_z(CO)$. The stoichiometry with respect to copper remains to be ascertained.

Dimerization Studies of $Cu(CO)_3$. Evidence for $Cu_2(CO)_6$. When a CO-Ar matrix containing mainly $Cu(CO)_3$ is allowed to warm up to temperatures at which the matrix is just beginning to break up and sublime off, the absorbances of the infrared lines of $Cu(CO)_3$ decrease rapidly with the concomitant growth of two new lines to slightly higher frequencies at 2039 and 2003 cm^{-1}. The two new lines continue to grow in during the warm-up process and at all times retain the same relative intensities. Eventually $Cu(CO)_3$ disappears, leaving broad absorptions belonging to the new species. These results suggest therefore that, as the matrix breaks up, the bulky $Cu(CO)_3$ residues gain some mobility and begin to diffuse. Bimolecular encounters must occur *before* decomposition, the result being dimerization to $Cu_2(CO)_6$. A Cu-Cu bonded structure is suggested as bridge CO modes were not observed. The presence of two CO stretching modes for $Cu_2(CO)_6$ in CO as well as in Ar is consistent with a D_3 rotameric configuration rather than the more highly symmetrical D_{3h} or D_{3d} configurations.

Copper Concentration Studies in CO Matrices. The Dependence of the Concentration of Binuclear Species on Metal-Matrix Gas Ratio. Further Evidence for $Cu_2(CO)_6$. Although it is possible, in principle, to detect the metal-metal stretching vibration belonging to molecules of the type $M_2(CO)_n$ using matrix Raman spectroscopy and to detect the electronic absorption band that can be assigned to a σ-σ^* transition between orbitals of the metal-metal bond using uv-visible spectroscopy (see later), it is interesting to try to discover other ways of identifying which bands in the ligand-stretching portion of the spectrum belong to binuclear metal species.

One technique that has been used successfully by us[13,17] is to investigate the relative absorbances of bands as a function of metal-matrix gas ratio. Binuclear species can arise in the matrix in two ways. The first is statistical, that is, metal dimers arising from the finite and calculable probability that in one of the nearest neighbor sites about a metal atom there resides another metal atom, while the second is due to reactions in the surface region of the matrix during the first few moments following deposition and before the kinetic energy of the reagents has been accommodated, hence while the molecules are still fairly mobile.

We have shown previously that both of these mechanisms give rise, at least in the case of metal atoms deposited into a "reactive matrix" and under such circumstances that mononuclear species still predominate, to binuclear species whose concentration is proportional to the square of the metal-matrix gas ratio, while the concentration of mononuclear species is directly proportional to that ratio. In fact our results to date[13,17] indicate that, at least in the case of first-row transition metals, the surface reaction mechanism far exceeds in importance the statistical generation of dimers. In brief, consider the matrix reaction between a metal atom M and CO which gives rise to mononuclear carbonyls $M(CO)_n$ where n = 1, 2, or 3 and binuclear species $M_2(CO)_m$ where, for example, m = 1-6 as in the case of the Cu-CO system. Species containing higher aggregates of metal are in general also possible. We will assume, however, that the matrix ratio, $[M]_0$, never becomes high enough to result in the formation of appreciable quantities of these. Let us now consider the surface reaction and the statistical factor separately.

Surface Reaction. We assume that only CO and M are mobile species. Accordingly only those reactions which involve at least one mobile species will be admitted. This implies that reactions of the form

$$M(CO)_n + M(CO)_{n'} \longrightarrow M_2(CO)_{n+n'}$$

are inadmissible. The total reaction scheme for the formation of $M(CO)_3$ and $M_2(CO)_6$ is shown in Scheme I. The

Scheme I

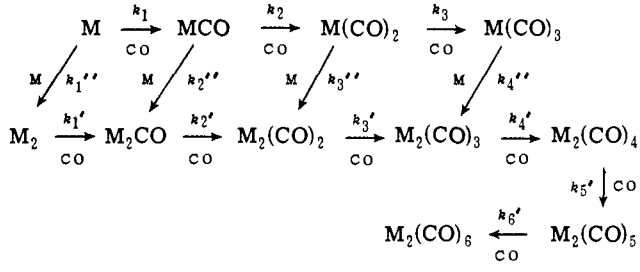

backward steps in these reactions are assumed to be negligibly slow and are thus not considered. The details of this analysis have been reported earlier[13,17] and can be summarized in the following equation

$$[M_2(CO)_6]/[M(CO)_3] = K[M]_0$$

where $[M]_0$ is the initial metal concentration and K is a constant. A similar analysis for metal trimers indicates that the analogous ratio involving trinuclears increases as the square of the metal-to-CO ratio.

Statistical Concentrations of Dimers. Assuming that aggregates larger than dimers are in negligible abundance and that there are 12 nearest neighbor sites associated with every substitutional site in the CO matrix, one can write down the metal dimer and metal monomer concentrations directly.

$$[M_2(CO)_6] = 12([M]_0^2)(1 - [M]_0)^{11}$$

$$[M(CO)_3] = [M]_0(1 - [M]_0)^{12}$$

and

$$[M_2(CO)_6]/[M(CO)_3] = 12[M]_0/(1 - [M]_0)$$

which reduces to approximately $12[M]_0$ for $[M]_0$ not too large.

We see therefore that both the statistical and surface reaction pathways lead to binuclear-mononuclear concentration ratios which are proportional to the matrix ratio while the appropriate ratios related to species containing larger metal aggregates vary as some higher power of the matrix ratio. It is therefore apparent that one can distinguish binuclear species from both higher aggregates and mononuclears by observing the effect of varying the matrix ratio on the relative absorbances of the appropriate spectral bands.

Using these techniques we undertook a study of the Cu-CO matrix reaction as a function of the Cu:CO ratio in the range 1:1000 to 1:100,000. The results of such a series of experiments are shown in Figure 5 and show quite clearly that at low Cu:CO ratios ($\leq$1:1000) $Cu(CO)_3$ is the only observable species on deposition. However, at higher Cu:

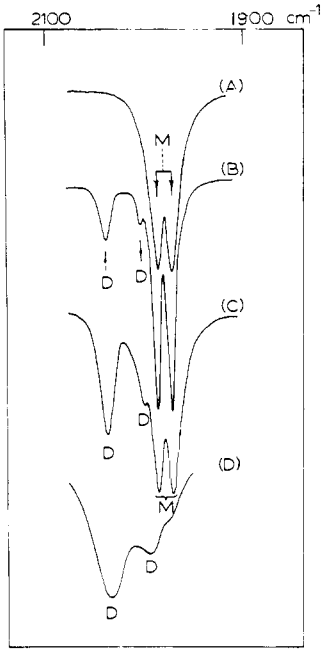

Figure 5. The infrared spectrum of the products of the matrix cocondensation reaction of copper atoms with pure CO at 15°K where the Cu:CO ratio increases on passing from A to D where M = $Cu(CO)_3$ and D = $Cu_2(CO)_6$ absorptions.

CO ratios (≥1:1000) two new lines (D) begin to grow in at 2039 and 2003 cm^{-1}, coincident with the lines ascribed to $Cu_2(CO)_6$ formed in the dimerization of $Cu(CO)_3$ in Ar matrices. At Cu:CO ratios approaching 1:100, the infrared absorbances of $Cu(CO)_3$ are hardly observable. Instead, the two new lines (D) dominate the spectrum.

The spectra shown in Figure 5 are plotted graphically in Figure 6 where a proportional increase in the absorbance ratio D/M is observed with increasing Cu concentrations. These results provide convincing evidence for the binuclear formulation $Cu_2(CO)_6$ for species D.

In summary, the infrared isotopic spectra, the Cu concentration dependence, and the formation of the new copper carbonyl species on allowing $Cu(CO)_3$ to diffuse suggest a dimerization process with the formation of a binuclear $Cu_2(CO)_6$ complex having a structure containing a copper-copper bond.

Mixed Metal Studies. If the product of a matrix cocondensation reaction is suspected to contain more than a single metal atom then, in principle, simultaneous deposition of *two* different metals (chosen usually from the same group in order to maintain similar chemical properties and to avoid major structural changes in the trapped product) with the reacting gas can verify the metal stoichiometry and aid the vibrational assignments. It turns out that the Cu-CO system is amenable to such a mixed metal study, as the analogous reaction of Ag atoms with pure CO produces an infrared spectrum showing a doublet at 1967 and 1937 cm^{-1}, a situation virtually identical with that of copper tricarbonyl. Furthermore, the mixed $^{12}C^{16}O$-$^{13}C^{16}O$ isotopic spectra were closely similar to those of copper tricarbonyl, suggesting the complex be formulated as silver tricarbonyl.[16]

When approximately equimolar concentrations of Cu and Ag atoms were simultaneously codeposited with pure CO at low metal concentrations, the observed spectrum was simply a *superposition* of the infrared spectra of the pure copper and silver tricarbonyls. Additional lines that could be attributed to a complex containing both Cu and Ag atoms were not observed on deposition nor after warm-up,

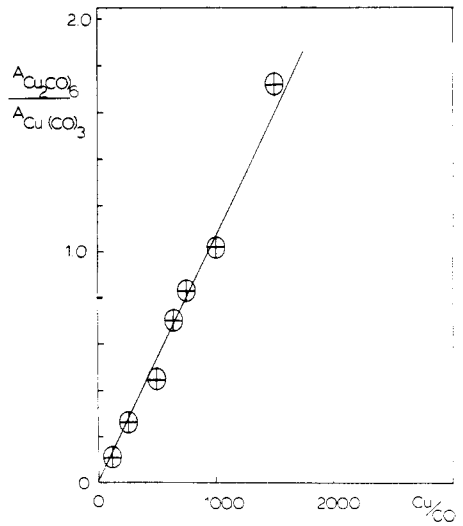

Figure 6. Graphical plot of the absorbance ratio $A_{Cu_2(CO)_6}/A_{Cu(CO)_3}$ as a function of Cu-CO.

reinforcing the view that the tricarbonyls are best formulated as mononuclear complexes, namely $Cu(CO)_3$ and $Ag(CO)_3$. The mononuclear formulation for $Cu(CO)_3$ has recently been confirmed by ESR spectroscopy.[45]

Copper Concentration Studies in Argon Matrices. Evidence for the Mononuclear Formulation of $Cu(CO)_2$ and Cu(CO). Consider the matrix reactions of Cu atoms and CO in Ar on deposition at *low* copper concentrations, under which conditions mononuclear carbonyls $Cu(CO)_n$ (where n = 1-3) are expected to predominate.

$$Cu \xrightarrow[CO]{k_1} Cu(CO) \xrightarrow[CO]{k_2} Cu(CO)_2 \xrightarrow[CO]{k_3} Cu(CO)_3$$

At intermediate CO:Ar ratios (1:10 to 1:100) where the ligand is in excess of the copper and all three species coexist, let us assume that the concentration of free CO is approximately constant. Under these circumstances the rate equations for the formation of mononuclear species *only* can be solved. The results of this analysis indicate that the absorbance ratios $A_{[CuCO]}:A_{[Cu(CO)_2]}:A_{[Cu(CO)_3]}$ should be independent of the copper concentration. A similar analysis performed in the presence of binuclear species is more complex but nevertheless indicates that the analogous ratio involving mononuclears should still be independent of the copper concentration.

It is therefore apparent that, having established that the product of the Cu-CO reaction at very low copper concentrations is the mononuclear tricarbonyl $Cu(CO)_3$, copper concentration studies can then be usefully employed to investigate the copper stoichiometry of the mono- and dicarbonyls formed in dilute CO-Ar matrices at low copper concentrations.

In our experiments the ratio of CO:Ar was chosen at 1:80, under which conditions the tri-, di-, and monocarbonyl complexes are all observable with reasonable absorbances. By studying the absorbances of these compounds as a function of Cu concentration, retaining the CO-Ar concentration constant, one discovers that the absorbance ratio $A_{[Cu(CO)_3]}:A_{[Cu_X(CO)_2]}:A_{[Cu_Y(CO)]}$ remains constant over a 300-fold change in Cu concentration, proving the new complexes to be mononuclear ($X = Y = 1$) with respect to copper, namely $Cu(CO)_2$ and Cu(CO).

Electronic Spectral Studies of Copper Atoms in Argon Matrices. Before discussing the electronic spectra of the products of the Cu-CO and Cu-CO-Ar matrix reactions, it is important to establish the fate of Cu atoms when deposit-

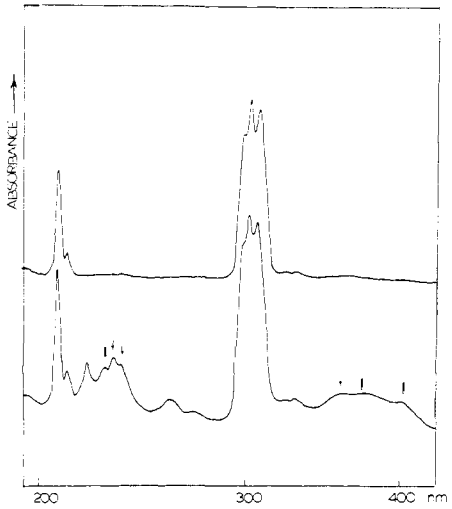

Figure 7. The uv-visible spectrum of (A) Cu:Ar ≃ 1:100,000 at 10°K showing the spectrum of matrix isolated copper atoms and (B) Cu:Ar ≃ 1:300 at 10°K showing in addition to atomic copper, new spectral features which can be assigned to Cu_n species (those marked with an arrow are assigned to Cu_2).

ed into argon at cryogenic temperatures. A number of metals have been isolated as atoms in inert matrices[18] in order to gain an insight into the effect of the matrix upon the spectra of trapped species and to study the diffusion mechanism of metal atoms and the possible formation of dimers in low temperature matrices. Apart from extremely light atoms such as Li[19] and Be[20] which diffuse readily in rare gas solids below 30°K, it has been proposed that heavier atoms such as Cu do not diffuse appreciably and aggregate after the deposition has been completed.[21] Matrix annealing with heavier atoms, after deposition, is supposed to have little effect other than causing the sharpening and/or shifting of spectral lines, usually attributable to the increasing regularity and/or phase changes in the matrix.

Several authors have reported on the electronic spectra of Cu atoms[18,21,47,48] trapped in matrices. Multiplet absorptions are observed, the centers of which are shifted to higher energies compared to the energy of the gaseous atom. A number of explanations have been offered to explain the above-mentioned effects, such as removal of orbital degeneracy by low matrix site symmetries, Jahn-Teller effects, interactions between pairs of trapped atoms on nonnearest sites in the host lattice, etc. Brewer et al.[22a] have used mixed metal codeposition studies in an attempt to discover the origin of the multiplet structure in the electronic spectrum of metal atoms. For example, 1 atom % of Ag atoms was simultaneously codeposited with Cu atoms.[22a] The atomic spectral lines remained essentially unperturbed, indicating that the fine structure was not due to nearest neighbor Cu-Cu interactions but rather site symmetry lattice perturbations. However, these data to not preclude the possibility that copper dimers or higher aggregates are formed, as originally suggested by Brewer and King[22a] and Meyer and Currie[22b] to account for weak features observed in the uv-visible spectra of Cu atoms in rare gas matrices at high metal concentrations.

In order to identify electronic lines originating from free Cu atoms under the conditions of our matrix experiments, we reinvestigated Cu atoms in Ar at Cu:Ar ≃ 1:100,000. Intense spectra were obtained after approximately 10-min depositions, a typical trace being shown in Figure 7A. The spectra were in close agreement with those previously reported.[18,21,47,48]

Spectral Evidence for Cu_2 Molecules in Argon Matrices.

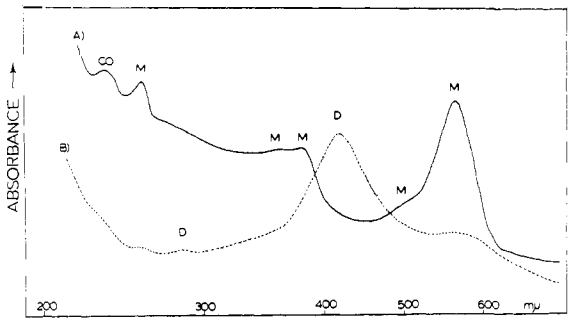

Figure 8. The uv-visible spectrum of the products of the matrix cocondensation reaction of copper atoms with pure CO at 10°K: (A) Cu:CO ≃ 1:10,000 showing $Cu(CO)_3$ (M), and (B) Cu:CO ≃ 1:100 showing $Cu_2(CO)_6$ (D).

The linear dependence of $A_{Cu_2(CO)_6}/A_{Cu(CO)_3}$ on Cu-CO (Figure 6) indicates that at *high* concentrations of copper (a) diffusion of Cu atoms on deposition, (b) dimerization to Cu_2 molecules and subsequent reaction to form $Cu_2(CO)_6$, and/or (c) reactions of Cu atoms with mononuclear species $Cu(CO)_n$ to form $Cu_2(CO)_6$ become favored processes. Consequently, we decided to investigate the electronic spectrum of copper in argon as a function of the Cu-Ar ratio in the range 1:10,000 to 1:100, in an attempt to establish the existence of Cu_2 molecules in inert matrices.

When Cu atoms were cocondensed with Ar at about 1:100,000, an extremely intense spectrum of atomic copper could be obtained after about a 10-min deposition (Figure 7A). Under these conditions, spectral lines assignable to Cu_n (where $n > 1$) were not apparent in the range 700-190 nm. However, a 300-fold increase in the concentration of copper, for example, was sufficient to cause a drastic reduction in the intensity of the atomic spectrum. Moreover, new spectral features appeared (Figure 7B) which could be attributable to Cu_n (where $n > 1$).

Using reasoning similar to that delineated earlier for the formation of binuclear carbonyl species, let us briefly consider the ways in which Cu_2 can arise in an argon matrix. As described earlier, the first is statistical, arising from the probability that in one of the 12 nearest neighbor substitutional sites about a Cu atom, there resides a single Cu atom. Thus

$$\frac{[Cu]_2}{[Cu]} = \frac{12[Cu]_0}{1 - [Cu]_0} \simeq K'[Cu]_0 \qquad (1)$$

where K' is a constant (for the matrix ratio $[Cu]_0$ not too large).

The second mechanism for the formation of Cu_2 is through reactions in the surface region of the matrix during matrix deposition. We will assume that in the matrix reactions which give rise to Cu_2, the matrix ratio $[Cu]_0$ never becomes sufficiently high to result in appreciable concentrations of aggregates higher than dimers. We assume that Cu is the only mobile species in the matrix. In the reaction

$$Cu \xrightarrow[Cu]{k_1} Cu_2$$

let us assume that the backward step is negligibly slow and is thus not considered, which leads to the ratio

$$\frac{[Cu_2]}{[Cu]} = k_1\tau_q[Cu]_0 \qquad (2)$$

where τ_q is the average quenching time of the matrix reaction.

The results of the analyses of the surface reaction at low copper concentrations and the statistical reaction both indicate that the ratio of the concentrations of $[Cu_2]/[Cu]$

Table V. Matrix Uv–Visible Spectrum of the Cu–CO Reaction Showing $Cu(CO)_3$ and $Cu_2(CO)_6$

Cu:CO ≃ 1:10,000 (nm)	Cu:CO ≃ 1:100 (nm)	Assignment
562 (s)		$Cu(CO)_3$
~495 (w sh)		$Cu(CO)_3$
	417 (s)	$Cu_2(CO)_6$
~375 (ms)		$Cu(CO)_3$
~344 (w sh)		$Cu(CO)_3$
	287 (w)	$Cu_2(CO)_6$
262 (w)		$Cu(CO)_3$

should increase proportionately to the matrix ratio $[Cu]_0$. Spectral lines which approximately show this behavior in the electronic spectrum of copper in argon are indicated in Figure 7B and are tentatively ascribed to Cu_2 molecules. Complete details of these Cu_n (n = 2, 3, ···) experiments will be reported in a forthcoming publication.[46]

Electronic Spectra of Copper Atoms in Carbon Monoxide and Carbon Monoxide–Argon Matrices. When Cu atoms were deposited into pure CO (1:10,000), a purple colored matrix was obtained. Uv-visible absorptions assignable to atomic copper were *not* observed. Instead a molecular spectrum of $Cu(CO)_3$ was observed, characterized by very intense broad absorptions (Figure 8A and Table V). At high Cu:CO ratios (1:100) a yellow matrix was obtained. A molecular spectrum entirely different from that of $Cu(CO)_3$ was observed (Figure 8B and Table V) and is assignable to $Cu_2(CO)_6$. On the other hand, spectral results at low copper concentrations and in dilute CO–Ar matrices (1:100 to 1:500) were completely different from the above, showing intense atomic copper lines as well as a structured low energy absorption which could be assigned to either $Cu(CO)_2$ or Cu(CO). The uv-visible spectral data for $Cu(CO)_3$ and $Cu_2(CO)_6$ are discussed in the following sections. However, as only one absorption at 660 nm could definitely be associated with $Cu(CO)_2$ and Cu(CO), which could be due to either low absorbance or overlap problems and/or the absorption lying outside of the accessible wavelength range of our spectrometer, we feel that the data are sufficiently incomplete not to merit further discussion.

The Molecular Orbital Description and Electronic Spectrum of $Cu(CO)_3$. In general, the observable electronic spectrum of carbonyl complexes $M(CO)_n$ can be subdivided into two main types, namely (i) transitions between levels primarily located on the metal and (ii) transitions between levels in which there is an electron transferred from the metal to the ligand, generally called "charge transfer". Transitions located mainly on the CO ligands, e.g., $\pi \rightarrow \pi^*$, are too high in energy to be observed in the easily accessible 190–700 mμ region.

The electronic spectrum observed for $Cu(CO)_3$ is relatively simple, showing two main absorptions at 562 and 375 nm and two weak shoulders at 495 and 344 nm, as well as a weak feature at 262 nm (Table V). Before concentrating on a detailed assignment of this spectrum, it is pertinent to obtain some ideas as to whether the observed transitions are of type i or ii or both. Let us briefly consider the predicted and observed trends in the metal → carbon monoxide charge transfer transitions in the series of complexes $Cr(CO)_6$, $Fe(CO)_5$, and $Ni(CO)_4$. In this series, the charge transfer band(s) would be predicted to move to higher energy as the effective nuclear charge on the metal increases, resulting from a stabilization of the metal orbital energies relative to the acceptor orbitals on the CO. (This trend is reflected in the valence orbital ionization potential of the metals.[24]) In addition, the charge transfer transition(s) would be expected to move to higher energies as the number of CO ligands donating charge to the central metal atom decreases; that is, the lower CO coordination number will be expected to stabilize the metal atom orbitals by virtue of a smaller spherical term repulsion between the metal and CO electron density.

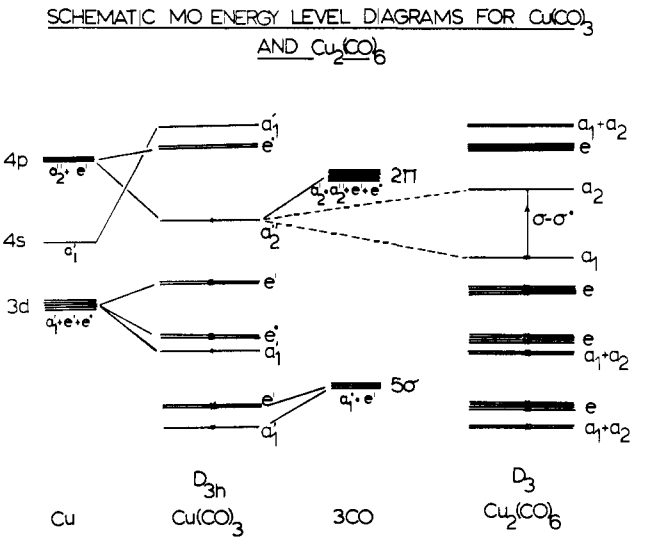

Figure 9. Qualitative molecular orbital energy level scheme for D_{3h}, $Cu(CO)_3$, and D_3, $Cu_2(CO)_6$.

This is the trend observed in practice: $Cr(CO)_6$ 44,480, 35,780 cm^{-1} (C.T.), and $Ni(CO)_4$ 52,130, 47,800 cm^{-1} (C.T.). However, one cannot extrapolate these data directly to $Cu(CO)_3$, as the lowest energy copper to CO charge transfer transition will now involve electronic excitation which is best described as 4s → π* (CO) rather than 3d → π* (CO). To obtain an insight into the spectral region where 4s → π* (CO) charge transfer transitions are likely to occur, one can use rough energy level schemes for $Cr(CO)_6$, $Ni(CO)_4$, and $Cu(CO)_3$.[23,24] Although the d → π* (CO) transitions in the copper complex are expected to be at much higher energies than in $Cr(CO)_6$ (the difference will be less pronounced when compared to $Ni(CO)_4$), some 24,000 cm^{-1} of this has to be subtracted to guess the energies of s → π* (CO) transitions for $Cu(CO)_3$. Hence, in the discussion and assignment of the electronic spectrum of $Cu(CO)_3$ (as well as the other copper carbonyls), the possibility of transitions between orbitals primarily located on the copper atom (s → p type) as well as copper to CO charge transfer (s → π* CO type) falling in the visible region must be taken into account.

To construct a qualitative molecular energy level scheme for $Cu(CO)_3$, we will use D_{3h} as the local symmetry of the copper atom. At the extreme left of Figure 9 the valence shell orbitals of Cu are shown with the symmetry labels appropriate to D_{3h} symmetry. Toward the extreme right of the diagram are the energy levels of the 5σ orbitals for the three CO groups also with symmetry designations appropriate to D_{3h}. The energy of the copper valence shell orbitals is assumed approximately equal to the appropriate valence orbital ionization potentials of atomic copper as given by Gray,[24] and the energies of the 5σ and 2π orbitals of CO were taken from the molecular orbital scheme reported by Mulliken.[25] The σ-bonding scheme is obtained by allowing copper and CO orbitals of the same symmetry type to interact where the energy level diagram is based purely on qualitative estimates of the relative energies of the molecular orbitals.

Account can be taken of the interaction of the Cu with the 2π orbitals of CO (which seems to occur, as the CO

stretching frequencies of $Cu(CO)_3$ indicate substantial Cu-C π-interactions) by finding the representations spanned by the six 2π orbitals of CO (shown with their symmetry designations toward the extreme right of the diagram) and allowing them to interact with the Cu orbitals of the same symmetry type. The molecular orbital energy level scheme resulting from this analysis is shown near the center of Figure 9 from which it can be seen that the highest filled molecular orbital in D_{3h} $Cu(CO)_3$ is of symmetry type a_2'' and contains a single electron. The electronic ground state is therefore expected to be $^2A_2''$.

The electronic spectrum of $Cu(CO)_3$ was recorded in a pure CO matrix and is shown in Figure 8A. The complex has deep purple color, the spectrum being dominated by two intense absorptions at 562 and 375 nm, with two much weaker shoulders at 495 and 344 nm. The two intense bands could be assigned to the $^2A_2'' \rightarrow {}^2A_1'$ and $^2A_2'' \rightarrow {}^2E''$ transitions, respectively, the former between orbitals which are mainly copper in character and the latter being a copper to CO charge transfer transition. The weak shoulders at approximately 495 and 344 nm most probably arise from a matrix site effect (see discussion of species 3 in CO matrices). Electronic transitions which are formally forbidden under D_{3h} could become slightly allowed in a matrix site of lower symmetry and could well account for the two shoulders at 495 and 344 nm.

It is difficult to decide on an unequivocal assignment of the electronic spectrum of $Cu(CO)_3$ with the present data alone. What is certain, however, is the credibility of Cu $\rightarrow$ π^* (CO) charge transfer occurring in the visible regions of the electronic spectrum of $Cu(CO)_3$.

Molecular Orbital Description and Electronic Spectrum of $Cu_2(CO)_6$. $Cu_2(CO)_6$ can be viewed as a dimer derived from two $Cu(CO)_3$ residues with the Cu-Cu single bond formed by overlap of the singly occupied, highest orbital of each $Cu(CO)_3$ unit as diagramed in Figure 9, analogous to the scheme proposed for $Mn_2(CO)_{10}$.[26] According to the infrared spectrum of $Cu_2(CO)_6$, the configuration adopted is probably that of D_3, and so we have used the appropriate symmetry designations for the electronic levels of the dimer. The electronic absorption spectrum of $Cu_2(CO)_6$ is dominated by an intense transition, λ_{max} 417 nm, which by analogy with Gray et al.[26] can be associated with the strongly allowed $^1A_1 \rightarrow {}^1A_2$ ($\sigma \rightarrow \sigma^*$) electronic transition involving orbitals arising from the copper-copper interaction. One other weaker absorption is observed for $Cu_2(CO)_6$ at 287 nm which by analogy with $Cu(CO)_3$ is tentatively assigned to the $^1A_1 \rightarrow {}^1E$ transition which is expected to shift to higher energy in the dimer, because of the stabilization of the $^1A_1$ ground state through the formation of the Cu-Cu bond. Poë et al.[27] have recently demonstrated that activation enthalpies for reactions of several metal–metal bonded carbonyls and bond stretching force constants for the metal-metal bond correlate well with the energies of an electronic absorption band that can be assigned to a σ-σ^* transition between orbitals of the metal-metal bond. Gray et al.[26] have made a rigorous assignment of the band at 343 nm in the electronic spectrum of $Mn_2(CO)_{10}$ to a σ-σ^* transition involving orbitals from the metal-metal interaction. Corresponding bands for $Tc_2(CO)_{10}$, $Re_2(CO)_{10}$, and $ReMn(CO)_{10}$ were also assigned by analogy ((σ-σ^*) nm): $Mn_2(CO)_{10}$ (343),[26,27] $Tc_2(CO)_{10}$ (316),[27] $Re_2(CO)_{10}$ (310),[27,28] $MnRe(CO)_{10}$ (324),[27] $Cu_2(CO)_6$ (417) (this study). These energies can be taken as an approximate measure of the energy required to break the metal–metal bond without drastically changing any of the other interactions in the molecule, and they should therefore provide some measure of the relative strengths of the M-M bonds. One is therefore led to believe that the extremely low σ-σ^* transition energy of $Cu_2(CO)_6$ compared to the σ-σ^* energies of other M-M bonded carbonyls (that are stable at room temperature) reflects a correspondingly low Cu-Cu bond dissociation energy (or Cu-Cu bond stretching force constant) and is consistent with the inability, so far, to synthesize the $Cu_2(CO)_6$ molecule by conventional chemical techniques.

Table VI. Frequency and Force Constant Calculations[a,b] for Isotopically Substituted $^lCu^mC^nO$ (where l = 63 or 65, m = 12 or 13, n = 16 or 18)

	Obsd frequency (cm^{-1})	Calcd frequency (cm^{-1})	Best Fit Force Constants (mdyn/Å)
$^{63}Cu^{12}C^{16}O$	2010.4	2010.9	
$^{63}Cu^{13}C^{16}O$	1966.5	1966.1	C-bonded Cu CO
$^{63}Cu^{12}C^{18}O$	1962.9	1962.7	f_r = 1.17
$^{65}Cu^{12}C^{16}O$	2008.3	2010.9	f_R = 16.67
$^{65}Cu^{13}C^{16}O$	1964.2	1966.2	f_{rR} = 0.63
$^{65}Cu^{12}C^{18}O$	1960.8	1962.7	
$^{63}Cu^{16}O^{12}C$	2010.4	2010.9	O-bonded Cu OC
$^{63}Cu^{16}O^{13}C$	1966.5	1966.1	f_r = 1.17
$^{63}Cu^{18}O^{13}C$	1962.9	1962.7	f_R = 16.59
$^{65}Cu^{16}O^{12}C$	2008.3	2010.9	f_{rR} = 0.54
$^{65}Cu^{16}O^{13}C$	1964.2	1966.1	
$^{65}Cu^{18}O^{12}C$	1960.8	1962.7	

[a] Note that a CK calculation yields f_R = 16.33 mdyn/Å. [b] ν(Cu–C) and ν(CuO) placed at 320 cm^{-1}.

Species 3 in Pure CO Matrices. Although the CO stretching modes of species 3 are considerably broader in CO matrices compared to Ar matrices, the $^{12}C^{16}O$-$^{13}C^{16}O$ experiment yielded a resolvable isotope pattern, the frequencies of which are listed in Table III. Apart from small matrix shifts and poorer resolution of the central doublet, the results in pure $^{12}C^{16}O$-$^{13}C^{16}O$ matrices are not very different from those obtained in argon (Table II and III). The warm-up data for species 3 in CO matrices show that within experimental error, the absorbance ratio of the 1990.0 and 1976.8 cm^{-1} doublet remained essentially invariant up to temperatures at which the matrix was beginning to sublime.

This contrasts sharply with the variable absorbance behavior of the 1985 and 1976 cm^{-1} doublet observed for species 3 in Ar, and described in an earlier section, indicating a more subtle explanation than a multiple trapping site for species 3 in solid CO. Intuitively one would expect that the perturbation would be caused by the CO molecules bonded to the copper, attempting to take up orientations similar to those that they would have in the carbon monoxide lattice. An examination of the reported crystal structure of CO[49] indicates that in pure CO matrices, the copper atom resides in the substitutional site where there are 12 nearest neighbors to every copper atom. Preferential interaction of the copper atom with three pseudo-triangular planar disposed nearest neighbor CO molecules is, then, the most favored scheme for the formation of $Cu(CO)_3$.

In the unsubstituted CO lattice, the three triangularly planar arranged CO molecules about any other CO have C_2 symmetry. It is reasonable to assume that the distortion of the three CO molecules bonded to the copper atom which is itself in a substitutional site in the CO lattice would be toward C_2. Judging from the proximity of the frequencies of the lines in Ar compared to CO, one concludes that the perturbation is slight but large enough, however, to remove the degeneracy of the E′ CO and CuC stretching modes, resulting in the observed doublet splitting in CO matrices.

It should be pointed out that distortion could occur either through the bending of the Cu—C skeleton or through the bending of the Cu—C≡O bonds. Whatever the case in practice it is possible to obtain an estimate of the angular distortion for $Cu(CO)_3$ in CO matrices by using the Cot-

ton-Kraihanzel[30] approximation and the intensity sum rules.[31] The expression

$$\frac{I_1 + I_2}{I_3} = \frac{1 + 2\cos^2\theta/2}{2\sin^2\theta/2}$$

is obtained where I_1, I_2, and I_3 are defined below.

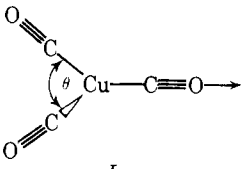

I_1
(A)
(not observed)

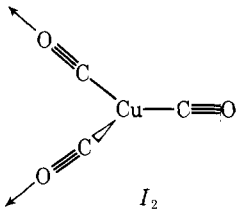

I_2
(A)
(1990.0 cm^{-1})

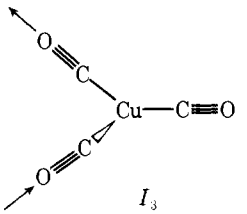

I_3
(B)
(1976.8 cm^{-1})

Assuming $I_1 \simeq 0$, and using the observed value of $I_2/I_3 = 0.941$, one calculates $\theta = 123°$.

Frequency Calculations for Isotopically Substituted Cu($^{12}C^{16}O)_n(^{13}C^{16}O)_{3-n}$ (where n = 0–3). The frequency calculations of the $^{12}C^{16}O$-$^{13}C^{16}O$-Ar mixed isotope data are greatly simplified if one assumes the Cotton-Kraihanzel approximation.[30] Since $Cu(CO)_3$ occurs in two sites (3 and 3_1), calculations based on D_{3h} symmetry were performed on both sites as follows. In the mixed isotope experiment one has to consider the formation of four possible complexes for each site (3 and 3_1 in Table II). However, one isotope line is missing, presumably because of an accidental overlap. This was established by performing a least-squares analysis of the isotopic data for the *four* observed lines of site 3 and the *three* observed lines of site 3_1, to yield the two sets of frequencies shown in Table II. The agreement between the observed and calculated frequencies for both sites is excellent for all observed CO stretching modes. It is particularly gratifying that the calculated frequency of the missing line of the tricarbonyl in site 3_1 (1943.0 cm^{-1}) suggests that it would be overlapped and hidden by the intense 1940.5-cm^{-1} line of the tricarbonyl in site 3. These calculations provide convincing evidence for the correctness of the $Cu(CO)_3$ assignment.

Frequency Calculations of Isotopically Substituted Cu($^{12}C^{16}O)_n(^{13}C^{16}O)_{2-n}$ (where n = 0–2). Using similar methods to those described above and a linear $D_{\infty h}$ geometry for $Cu(CO)_2$, one has to consider the formation of the three possible mixed isotopic molecules listed in Table IV. A least-squares analysis was again performed on the isotopic data obtained in argon (for both sites 2 and 2_1) to yield the two sets of four frequencies shown in Table IV. The agreement between the observed and calculated modes was again excellent and supports the $Cu(CO)_2$ two-site assignment. The in-phase high frequency CO stretching mode of Cu($^{12}C^{16}O$)($^{13}C^{16}O$) was calculated to occur at about 1995.0 cm^{-1} and was presumably not observed because of its expected low absorbance. This contention is supported by isotope intensity calculations (Table IV).

A Feasibility Study of Distinguishing C-Bonded and O-Bonded Carbonyls from Frequency Calculations of Isotopically Substituted $^{l}Cu^{m}C^{n}O$ and $^{l}Cu^{n}O^{m}C$ (where l = 63 or 65, m = 12 or 13, n = 16 or 18). As described earlier, synthesis of spectroscopically pure copper monocarbonyl can be achieved in Cu:CO:Ar ≈ 0.1:1:500 mixtures. The infrared spectrum displays a closely spaced doublet at 2010.4 and 2008.3 cm^{-1}. Two questions remain to be answered. Firstly, does the doublet splitting originate from a copper isotope effect (^{63}Cu, 69.1%; ^{65}Cu, 30.9%) or a matrix multiple trapping site effect? Secondly, is it possible to unambiguously establish the mode of bonding of the CO to the Cu from a combination of copper and carbon monoxide isotopic substitution?

It turns out, that an insight into both problems can be obtained from $^{12}C^{16}O$:$^{13}C^{16}O$:$^{12}C^{18}O$:Ar ≃ 1:1:1.5:1500 triple isotope experiments using natural copper (Figure 4, Table VI). Unfortunately, copper monocarbonyl, like many other matrix isolated carbonyls, has an extremely low intensity copper-carbon stretching mode compared to the corresponding CO stretching mode. Considerable efforts were spent searching for the Cu-C stretching mode in the 500-200-cm^{-1} region, without success. However, warm-up experiments were somewhat informative, indicating that a very weak band in the region of 320 cm^{-1} could be the mode in question.

Assuming the following assignments ($^{63}Cu^{12}C^{16}O$, 2010.4 (ν(CO)); $^{63}Cu^{13}C^{16}O$, 1966.5 (ν(CO)); $^{63}Cu^{12}C^{18}O$, 1962.9 (ν(CO)); $^{63}Cu^{12}C^{16}O$, 320.0 cm^{-1} (ν(CuC))) a normal coordinate calculation was performed for a linear C-bonded carbonyl, the parameters f_r, f_R, and f_{rR} being adjusted to yield the best fit frequencies and force

$$\overset{r}{Cu}—\overset{R}{C}\equiv O$$

constants (Table VI). The fit was acceptable for all four modes.

The force constants so obtained were then used to compute the frequencies of the three ^{65}Cu molecules. The results immediately demonstrated (Table VI) that the observed 2.1-cm^{-1} doublet splitting of copper monocarbonyl is too large to be acceptable as a copper isotope effect and is more in keeping with a multiple trapping site rationalization. This conclusion receives convincing support from the observation of a single absorption at 2012.0 cm^{-1} for copper monocarbonyl in dilute CO-Kr matrices. Furthermore, the close correspondence between the ^{63}Cu and ^{65}Cu calculated frequencies vindicates the usefulness of the Cotton-Kraihanzel approximation.

The calculations described for CuCO were repeated for an O-bonded model with the CuO stretching mode likewise

$$\overset{r}{Cu}—\overset{R}{O}\equiv C$$

assumed to be in the 320-cm^{-1} region. Not unexpectedly, the computed fits for the O-bonded model were as close as those for the C-bonded model. One is therefore forced to conclude that even with high quality ^{63}Cu, ^{65}Cu, $^{12}C^{16}O$, $^{13}C^{16}O$, and $^{12}C^{18}O$ isotopic data, one cannot draw meaningful conclusions regarding the mode of bonding of the CO ligand to the copper atom.

Conclusion

The discovery of thermally unstable copper carbonyls can be considered to add a new dimension to our knowledge of the binary carbonyls of the first transition series. Historically speaking, our data may be considered to authenticate some of the very early claims[1-6] of unstable copper carbonyls which were postulated to exist in the vapors of copper transported by streams of heated CO.

Clearly, the generally held view for the nonexistence of binary copper, silver, and gold carbonyls, namely the stabilities of the filled nd^{10} valence shells (a situation not con-

ducive to d_π-π^* back-bonding) is no longer tenable as the observed CO stretching modes for the complexes occur in the region 2050-1800 cm^{-1}. These CO frequencies are by no means abnormal for binary carbonyls (cf. $Ni(CO)_4$, $\nu(CO)(T_2)$ = 2050 cm^{-1}) and denote a substantial d_π-π^* contribution to the overall M-CO bonding. However, the metal-carbon stretching frequencies (ν(Cu-C) = 375-325 cm^{-1}; ν(Ag-C) ~ 250 cm^{-1} [16] and ν(Au-C) < 200 cm^{-1} [42]) are anomalously low and imply a substantially weaker M-C interaction than in $Ni(CO)_4$ ($\nu(NiC)(T_2)$ = 435 cm^{-1}), consistent with the low thermal stability of $Cu(CO)_n$, $Ag(CO)_n$, and $Au(CO)_m$ (where n = 1-3, m = 1-2).

The statistical generation of mononuclear and binuclear complexes as well as their production from reactions in the surface region during matrix deposition have both been analyzed in terms of the metal/matrix ratio. Both pathways are shown to lead to binuclear/mononuclear concentration ratios which are proportional to the matrix ratio and as much indicate that metal concentration studies should prove to be an invaluable technique for future studies involving metal atoms in chemical synthesis.

Acknowledgments. We wish to thank the National Research Council and the Research Corporation for grants in aid of research.

References and Notes

(1) H. Kunz-Krause, *Apoth. Ztg.*, **31**, 66 (1916).
(2) V. A. Plotnikov and K. N. Ivanov, *Zh. Khim. Promsti.*, **7**, 1136 (1930); V. A. Plotnikov and O. K. Kudra, *Zh. Obshch. Khim.*, **1**, 1075 (1931).
(3) D. A. Pospekhov, *Zh. Prikl. Khim.*, **19**, 848 (1946).
(4) C. R. Bertand, *C. R. Acad. Sci.*, **177**, 997 (1923).
(5) E. Mond and C. Heberlein, *J. Chem. Soc.*, **125**, 1222 (1924).
(6) E. H. Boomer, H. E. Morris, and G. H. Argue, *Nature (London)*, **129**, 438 (1932); F. Körösy, *ibid.*, **160**, 21 (1947); A. Keller and F. Körösy, *ibid.*, **162**, 580, 1948; J. G. Maltby, *ibid.*, **160**, 468 (1947); A. Keller, *ibid.*, **167**, 907 (1951); H. Bloom, *ibid.*, **159**, 539 (1947).
(7) R. P. Elschens, W. A. Pliskin, and S. A. Francis, *J. Chem. Phys.*, **22**, 1986 (1954); J. Pritchard, *Trans. Faraday Soc.*, **59**, 437 (1963); J. Pritchard and M. L. Sims, *ibid.*, **66**, 427 (1970).
(8) F. A. Cotton and T. J. Marks, *J. Am. Chem. Soc.*, **92**, 5114 (1970).
(9) G. A. Ozin and A. Vander Voet, *Acc. Chem. Res.*, **6**, 313 (1973).
(10) J. S. Ogden, *Chem. Commun.*, 978 (1971).
(11) E. P. Kündig and G. A. Ozin, *Progr. Inorg. Chem.*, in press.
(12) A. Kant and B. Strauss, *J. Chem. Phys.*, **41**, 3806 (1964).
(13) See, for example, L. Hanlan and G. A. Ozin, *J. Am. Chem. Soc.*, **96**, 6324 (1974); H. Huber, E. P. Kündig, G. A. Ozin, and A. J. Poë, *ibid.*, **97**, 308 (1975).
(14) E. P. Kündig, M. Moskovits, and G. A. Ozin, *J. Mol. Spectrosc.*, **14**, 137 (1972).
(15) M. Moskovits and G. A. Ozin, *J. Appl. Spectrosc.*, **26**, 481 (1972).
(16) E. P. Kündig, D. McIntosh, M. Moskovits, and G. A. Ozin, unpublished results.
(17) E. P. Kündig, M. Moskovits, and G. A. Ozin, *Angew. Chem., Int. Ed. Engl.*, in press.
(18) D. M. Mann and H. P. Broida, *J. Chem. Phys.*, **55**, 84 (1971).
(19) L. Andrews and G. C. Pimentel, *J. Chem. Phys.*, **47**, 2905 (1967).
(20) W. Weltner, private communication.
(21) L. Brewer and J. Wang, *J. Mol. Spectrosc.*, **40**, 95 (1971), and references therein.
(22) (a) L. Brewer and B. King, *J. Chem. Phys.*, **53**, 3981 (1970); (b) B. Meyer and Currie, unpublished data from ref 22.
(23) C. Moore, *Nat. Bur. Stand. (U.S.), Circ*, **No. 467** (1974).
(24) H. Basch, A. Viste, and H. B. Gray, *J. Chem. Phys.*, **44**, 10 (1966).
(25) R. S. Mulliken, *Can. J. Chem.*, **36**, 10 (1958).
(26) R. A. Levenson, H. B. Gray, and G. P. Ceasar, *J. Am. Chem. Soc.*, **92**, 3653 (1970).
(27) J. P. Fawcett, A. J. Poë, and M. V. Twigg, *J. Chem. Soc., Chem. Commun.*, 267 (1973).
(28) M. Wrighton and D. Bredesen, *J. Organomet. Chem.*, **50**, C35 (1973).
(29) R. G. Pearson, *J. Am. Chem. Soc.*, **91**, 4947 (1969).
(30) F. A. Cotton and C. S. Kraihanzel, *J. Am. Chem. Soc.*, **84**, 4432 (1962).
(31) E. B. Wilson, J. C. Decius, and P. C. Cross, "Molecular Vibrations", McGraw-Hill, New York, N.Y., 1955.
(32) R. Dekock, *Inorg. Chem.*, **10**, 1205 (1971).
(33) E. P. Kündig, M. Moskovits, and G. A. Ozin, *Can. J. Chem.*, **50**, 3587 (1972).
(34) J. H. Darling and J. S. Ogden, *J. Chem. Soc., Dalton Trans.*, 1079 (1973).
(35) E. P. Kündig, D. McIntosh, M. Moskovits, and G. A. Ozin, *J. Am. Chem. Soc.*, **95**, 7234 (1973).
(36) L. A. Hanlan, E. P. Kündig, H. Huber, M. Moskovits, and G. A. Ozin, *J. Am. Chem. Soc.*, in press.
(37) E. P. Kündig and G. A. Ozin, (unpublished work).
(38) T. A. Ford and G. A. Ozin, unpublished data.
(39) J. L. Slater, R. K. Sheline, K. C. Lin, and W. Weltner, Jr., *J. Chem. Phys.*, **55**, 5129 (1971).
(40) V. Calder, J. L. Slater, and T. C. DeVore, *Inorg. Chem.*, **12**, 1918 (1973).
(41) H. Huber and G. A. Ozin, unpublished data.
(42) D. McIntosh and G. A. Ozin, unpublished data.
(43) A. Bos, *J. Chem. Soc., Chem. Commun.*, 26 (1972).
(44) J. S. Ogden, A. J. Hinchcliffe, and D. D. Oswald, *J. Chem. Soc., Chem. Commun.*, 338 (1972).
(45) G. A. Ozin, E. P. Kündig, W. Weltner, and J. Wilkerson, unpublished data.
(46) E. P. Kündig and G. A. Ozin, in preparation.
(47) D. H. Carstens and D. M. Gruen, *Rev. Sci. Instrum.*, **42**, 1194 (1971).
(48) J. Shirk and A. M. Bass, *J. Chem. Phys.*, **49**, 5156 (1968).
(49) R. W. G. Wyckoff, "Crystal Structures", Vol. 7, Interscience, New York, N.Y., 1974, p 29.